LVRT Capability of Single-Phase Grid-Connected HERIC Inverter in PV Systems by a Look-up Table Based Predictive Control

Esmaeil Zangeneh Bighash and
Seyed Mohammad Sadeghzadeh
Faculty of Engineering
Shahed University
Tehran, Iran
Esmaeilzangane@gmail.com and Sadeghzadeh@shahed.ac.ir

Esmaeil Ebrahimzadeh and Frede Blaabjerg
Department of Energy Technology
Aalborg University
Aalborg, Denmark
ebb@et.aau.dk and fbl@et.aau.dk

***Abstract*- Nowadays capacity of the photovoltaic systems in the grid is remarkable and provides a major part of energy in the grid. Therefore, an abruption of these systems from the grid can create a damage to the grid. Unlike in the past that PV systems disconnected from the grid when a voltage drop occurred, nowadays these systems should have Low Voltage Ride-Through (LVRT) capability. The PV system should stay connected to the grid at fault time and help to recover the grid voltage by injecting the reactive power like in a power plant or a custom power device. There are two important factors for single phase grid connected PV inverters. The first one is the structure of the inverter and the second one is the control part. In this regard, the HERIC inverter can be a good selection among the transformerless inverters for a PV system due to its high efficiency. For the control part, this paper presents a look-up table based Model Predictive Control (MPC) that is simple, fast and has soft behavior in tracking of the reference during LVRT. The proposed control method has been implemented in a 1 kW single-phase transformerless HERIC (Highly Efficient and Reliable Inverter Concept) inverter using an LCL filter.**

Keyword— ***Model Predictive Control (MPC); Photovoltaic (PV); Low Voltage Ride-Through (LVRT).***

I. INTRODUCTION

In the last decades, the capacity of PV systems in the utility grid is dramatically increased [1]. Therefore, these systems have created some concerns about their effects on the power quality and reliability of the grid [2-4]. For example, based on current standards for PV systems when a voltage sag occurs the PV system should disconnect from the grid and stop injecting power to grid. However, due to the high capacity of these systems in the grid, abruption of injecting power can create a shock to system and even help to fault and finally deteriorate of the current situation [5-6]. In this regard, some countries have updated their grid code standards. In these standards, the PV system should stay connected during the voltage sag period and helps to recover the voltage by injecting reactive power [7-10].

Recently, some papers have studied the PV systems with LVRT capability e.g.[11-14]. In [11] a benchmark of grid fault modes has been studied for future single-phase PV systems. In [12], a synchronization method for single-phase grid-connected photovoltaic systems under grid faults is also introduced. In [13], the authors worked on modelling and control of three phase PV systems with respect to the German grid code by using a positive sequence current control in order to operate during LVRT. In [14] a transformerless single-phase grid connected inverter with LVRT capability has been controlled by using a classical PR controller.

This paper presents a Model Predictive Control (MPC) based on a look-up table that is to easy implement, robust, and has fast dynamic response and soft behavior. In the proposed current control method, the final control switching will be determined by a cost function. To increase the accuracy and adaptability of MPC in a single phase inverter, some virtual vectors are applied by using a switching table.

The paper is organized as follows: first a summary of selected transformerless inverter is explained. Then the paper focus on reactive power strategy in the LVRT mode. In section IV, the proposed control method for a single-phase PV system is presented. Finally, before the conclusions simulation results of the proposed controller are given and analyzed.

II. TRANSFORMERLESS PV-INVERTERS

As the efficiency is one of the most important factors for PV systems, transformerless inverters are widely used. Different structures for single-phase transformerless PV inverters have been presented [15]. Among them, the Highly Efficient and Reliable Inverter Concept (HERIC) has the highest efficiency [16], which is selected in this paper to be connected to the utility grid.

Also, the LCL filters are widely used at the output of these inverters. The LCL filter attenuates high-frequency harmonics better than the L filter and can also be used in both standalone systems and grid-connected systems [17-20].

One of the newest structures of the single-phase grid-connected PV inverters, which has a low leakage current and high efficiency is the HERIC inverter with an LCL filter. The proposed PV structure has two stages which are a DC/DC converter and a DC/AC inverter as shown in Fig. 1.

978-1-5386-1127-2/17/$31.00 ©2017 IEEE

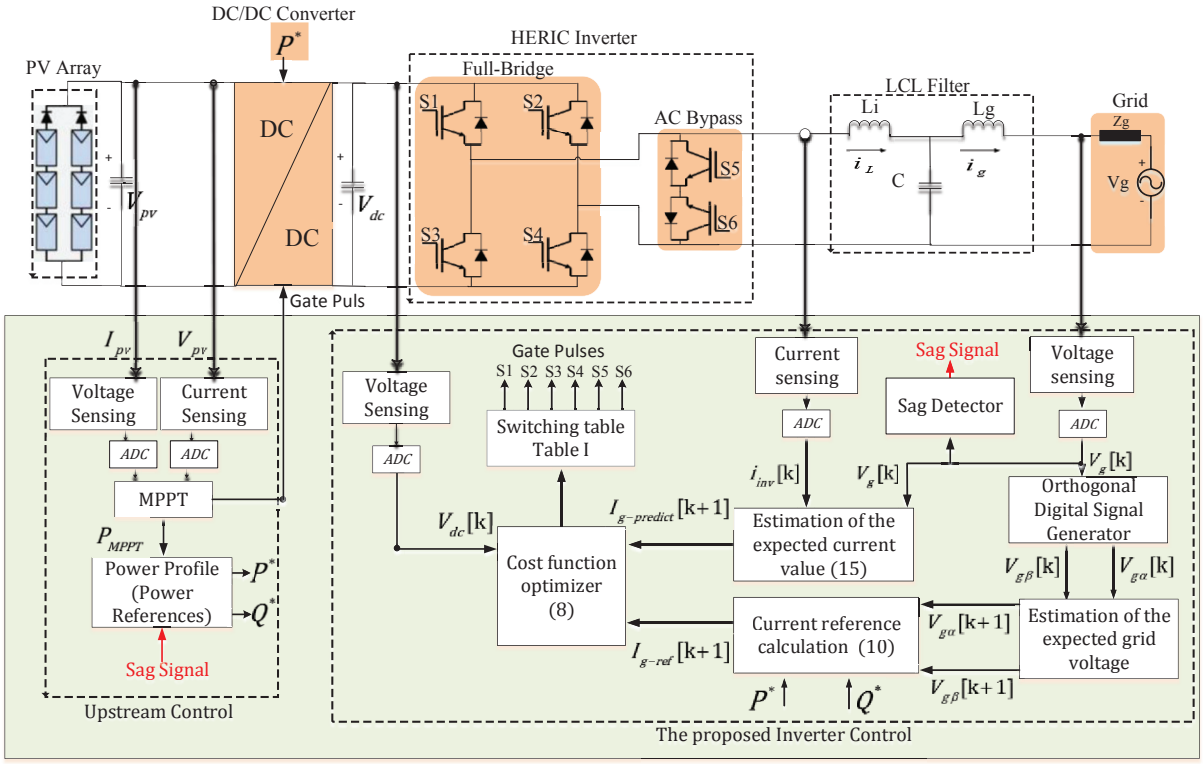

Fig. 1. Proposed MPC control block diagram of single phase HERIC inverter with LVRT capability.

III. Reactive Power Strategy in LVRT

Fig. 2 and Fig. 3 show the relationship between reactive power and voltage in LVRT duration in the German grid code [13] and [21]. Fig. 2 shows the profile of Low Voltage Ride-Through that has been forced in some countries for grid connected inverters. According to the Q-V profile in Fig. 3, depending on the grid voltage, reactive power reference (Q^*) is calculated and should be injected into the grid. Some reactive power control strategies are proposed in [9] and among them, two important strategies are selected as it will be explained in following.

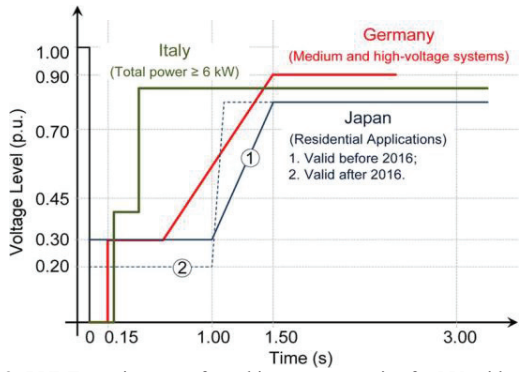

Fig. 2. LVRT requirements forced in some countries for PV grid connection [14],[21].

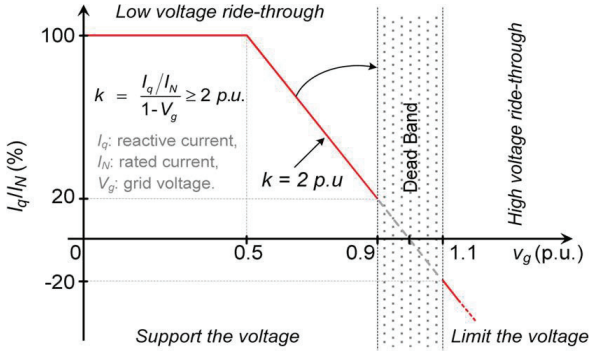

Fig. 3. Reactive current injection requirements in E.ON grid code [5], [13].

A. Constant Peak Current strategy

In this strategy, the inverter will not be overcurrent when injecting the reactive power in addition active power in LVRT period. Two components I_d and I_q determine the active and reactive power references. I_d is related to active power coming from the Maximum Power Point Tracker (MPPT) and I_q is related to reactive power determined from the LVRT controller. In this case, I_d and I_q can be obtained as

$$\begin{cases} I_q = k\left(1 - v_{gm}\right) I_N \\ I_d = \sqrt{{I_{g\,max}}^2 - {I_q}^2} \end{cases} \quad (1)$$

$$I_{g\max} = I_N = \sqrt{{I_d}^2 + {I_q}^2} \quad (2)$$

where v_{gm} is the per unit of the grid voltage amplitude and I_N is the nominal current of the inverter and $k \geq 2$. It can be seen from Fig. 3 that the PV inverter should only inject reactive power ($I_q = I_{g\,max}, I_d = 0$) when $v_{gm} < 0.5$. The power references of the inverter can be calculated by the following equation.

$$\mathrm{P}^* = \frac{1}{2} V_d I_d \quad (3)$$

$$Q^* = \frac{1}{2} V_d I_q \quad (4)$$

The PV systems have two stages, DC/DC converter and the inverter. The DC/DC converter extracts the maximum power from the panels to the DC link by using MPPT algorithm. However, for the LVRT condition, P^* is determined from the LVRT unit, such that the DC/DC converter should exit from the MPPT processing and deliver active power reference (P^*) determined from the LVRT unit.

B. Constant Active Power strategy

This strategy is implemented to gain the maximum power from the panels and the DC/DC converter to stay in the MPPT processing in LVRT mode. Therefore, unlink the constant peak current strategy that decrease the active power reference during injecting the reactive power in order to protect from overcurrent, in this strategy even during the LVRT the active power reference is equal to the MPPT reference. I_d and I_q are calculated by:

$$\begin{cases} I_q = k\left(1 - v_{gm}\right) I_N \\ I_d = I_{d-MPPT} \end{cases} \quad (5)$$

When v_{gm}< 0.5 the inverter should inject completely reactive power ($I_q = I_{g\,max}, I_d = 0$) as given in the standards.
Although this strategy extracts the maximum power from the panels even in the LVR period, but it makes an overcurrent for the inverter and maybe shutdown.

IV. The Proposed model predictive control

A. Modeling of the power stage

In Fig. 1, $L_i, L_g, and\ C$ are the inverter side inductor, the grid side inductor, and the capacitor of the LCL filter, respectively. $V_g(t)$ is the grid voltage, $V_{dc}(t)$ is the dc-link voltage, and $V_{inv}(t)$ is the output voltage of the inverter. Due to [22], the LCL filter can be approximated as an L filter ($L = L_i + L_g$) if the LCL filter is designed according to

$$f_p = \frac{1}{2\pi\sqrt{LC}} > f_c \quad (6)$$

where f_c is the control crossover frequency and f_c is the parallel resonant frequency. This is a valid dynamic approximation if the control bandwidth is kept below f_p.

1) The principle of the proposed MPC controller

The grid current is controlled by a cost function, which is defined as

$$g = \left| i_{g\_ref}[\mathrm{k+1}] - i_{g\_\mathrm{Predict}}[\mathrm{k+1}] \right| \quad (7)$$

where $i_{g\_ref}[k+1]$ is the next sample of grid current reference and $i_{g\_Predict}[k+1]$ is calculated and estimated by the system model, which is presented in the next sections.

2) Calculation of the next sampling of the grid current ($i_{g\_ref}[k+1]$)

In the photovoltaic systems, during the normal operation, the active power reference is determined by MPPT algorithm and reactive power will be set to zero. But depending on the voltage sag, the amount of reactive power reference can be calculated from a constant peak current and constant active power strategies. Therefore, after determining P^*, Q^*reference, the next sample current reference to achieve $\mathrm{P}^*$and Q^* is determined from equation (8).

$$i_{g\_\mathrm{ref}}[\mathrm{k+1}] = \frac{2}{v_{g\alpha}[\mathrm{k+1}]^2 + v_{g\beta}[\mathrm{k+1}]^2} * \begin{pmatrix} V_{g\alpha}[\mathrm{k+1}] & V_{g\beta}[\mathrm{k+1}] \end{pmatrix} \begin{bmatrix} P^* \\ Q^* \end{bmatrix} \quad (8)$$

where $V_{g\alpha}[k+1]$ and $V_{g\beta}[k+1]$ are the orthogonal components for the next sample of the grid voltage, which are calculated by Orthogonal Digital Signal Generator (ODSG) algorithm as presented in [23].

3) Calculation of the estimated current ($i_{g\_Predict}[k+1]$)

To calculate $i_{g\_Predict}[k+1]$, the inverter in Fig. 1 can be modeled by the following equations.

$$V_{inv}(\mathrm{t}) = V_g(\mathrm{t}) + \mathrm{L}_i \frac{di_L(\mathrm{t})}{dt} + \mathrm{L}_g \frac{di_g(\mathrm{t})}{dt} \quad (9)$$

Assuming that the inverter works with a fixed frequency, the switching time (T_s) is constant. Rewrite (9) in discrete-time domain and employing an Euler equation,

$$V_{inv}[\mathrm{k}] = V_g[\mathrm{k}] + \mathrm{L}_i \frac{I_L[\mathrm{k+1}] - I_L[\mathrm{k}]}{T_S} + \mathrm{L}_g \frac{I_g[\mathrm{k+1}] - I_g[\mathrm{k}]}{T_S} \quad (10)$$

where $V_{inv}[k]$, and $V_g[k]$ are the inverter output voltage and the grid output voltage over the switching period $[k, k+1]$. $I_L[k]$

and I_g [k] are the inverter side current and the grid side current at the sampling point of [k].

According to the dynamic approximation of the LCL as an L filter, equation (10) can be rewritten to

$$i_{g\_\text{Predict}}[\text{k+1}] = \frac{T_S}{(\text{L}_i + \text{L}_g)}\left(\text{V}_{inv}[\text{k}] - V_g[\text{k}]\right) + i_g[\text{k}] \qquad (11)$$

B. Switching strategy in the proposed MPC controller

The switching states in the HERIC inverter can be shown as a function of S_a, S_b and S_c by the following equations.

$$S_a = \begin{cases} 1, S_1 = 1 \,\&\, S_3 = 0 \\ 0, S_1 = 0 \,\&\, S_3 = 1 \end{cases}$$

$$S_b = \begin{cases} 1, S_2 = 1 \,\&\, S_4 = 0 \\ 0, S_2 = 0 \,\&\, S_4 = 1 \end{cases} \qquad (12)$$

$$S_c = \begin{cases} 1, S_5 = 0 \,\&\, S_6 = 0 \\ 0^+, S_5 = 0 \,\&\, S_6 = 1 \\ 0^-, S_5 = 1 \,\&\, S_6 = 0 \end{cases}$$

The state 0^+ is the zero state for the freewheeling mode of HERIC inverter in positive cycle and State 0^- is the zero state for freewheeling mode in negative cycle. The HERIC inverter switching space vector equation comes from (13).

$$S = (\text{S}_a + \text{aS}_b)\text{S}_c \qquad (13)$$

Where $a = e^{j\pi}$ and the inverter output voltage is defined as given in equation (14).

$$V_{inv} = SV_{dc} \qquad (14)$$

The proposed switching space vectors for a single phase HERIC inverter is defined as $V_s(S_a, S_b, S_c)$. Where all of these vectors for HERIC inverter are shown in Fig. 4.

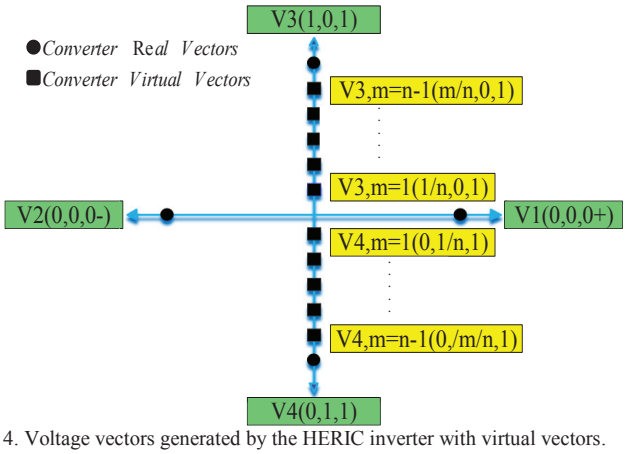

Fig. 4. Voltage vectors generated by the HERIC inverter with virtual vectors.

1) Vector selection and applying vectors

The proposed switching vectors in the proposed method are shown in Fig. 4. The vectors in the MPC are including four basic or real vectors (the circle symbols in Fig.4) and several virtual vectors (the square symbols in Fig.4). The number of virtual vectors can be increased as far as the THD is within standard limit. The virtual vectors are generated by a switching table with a combination of the basis vectors as table I.

2) Determination of the inverter voltage reference

In the proposed MPC method, the inverter reference voltage can be given as

$$V_{inv} = \frac{m}{n} V_{dc} \qquad (15)$$

where $\underline{n}$ is the number of vectors and $\underline{m}$ varies from 1 to $\underline{n}$. All values of V_{inv} in equation (15) will be placed in equation (11) and $i_{g\_Predict}$ is then calculated.

Then $i_{g\_Predict}$ is tested in a cost function. Any amount of V_{inv} that minimizes the cost function is the inverter reference (V_{inv}^*) and will determine the duty cycle time (T_d) for the modulation part.

$$T_d = \frac{V_{inv}^*}{V_{dc}} T_S, \text{or}, \text{T}_d = \frac{m}{n} T_S \qquad (16)$$

3) Modulation in the proposed MPC

After determining of the V_{inv}^* vector, this vector is applied by the proposed switching table given in Table I. In this case, the selected vector by (15) will be applied during T_d and then a zero vector should be applied for zero time (T_0).

Where $T_0 = T_S - T_d$ (16)

Table I shows more details of the switching table for applying the vectors in the proposed MPC.

TABLE I
Look-up table for applying vectors in the proposed MPC

Detected sectors	Selected vector	T_s	
		T_d	T_0
Positive	$V_{3,m}$	V_3 (1,0,1)	V_1 (0,0,0+)
Negative	$V_{4,m}$	V_4 (0,1,1)	V_2 (0,0,0-)
Zero	V_1	V_1 (0,0,0+)	
	V_2	V_2 (0,0,0-)	

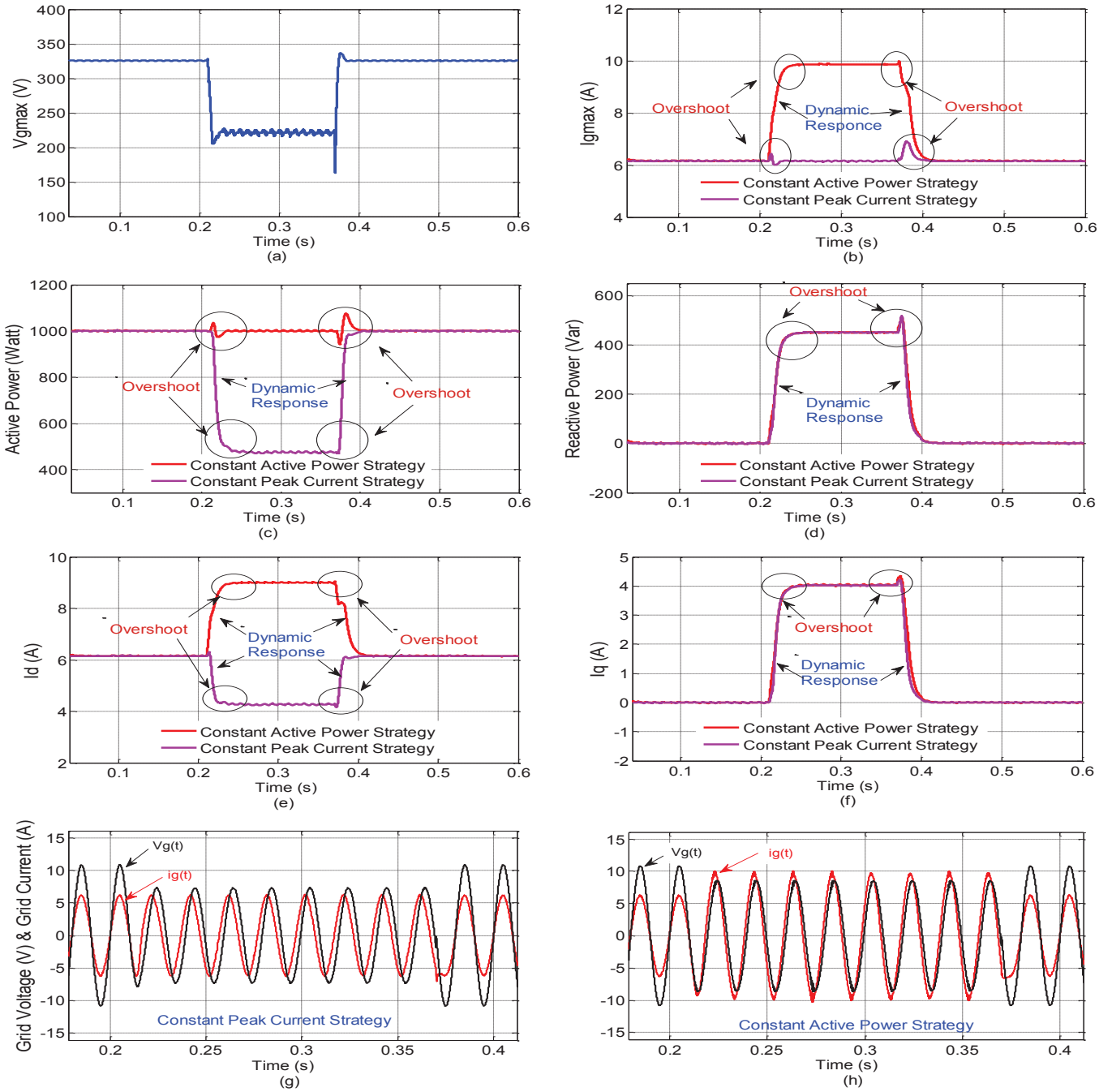

Fig. 5. Simulation results of single phase grid connected HERIC inverter by the proposed MPC method: (a) and (b) and the maximum of grid voltage and current, (c) and (d) injected active and reactive powers, (e) and (f) injected current in dq-domain, (g) and (h) grid voltage and current in both reactive power strategy.

V. SIMULATION RESULTS

Simulations have been done in MATLAB Simulink. The simulation parameters are given in Table II.

Simulations have been done for two control strategies, constant peak current mode and constant active power strategy. In the first one, simulation has been done to force the inverter to stay in constant peak current and for the second one, the control

system force the inverter to inject constant active power during LVRT.

TABLE II
Simulation parameters of HERIC

Description	Value
Grid Frequency	$\Omega = 2\pi \times 50$ rad/s
Grid Voltage	Vg= 220 V
Rated Power	Pn=1 kW
DC-bus voltage	Vdc=400 V
Switching Frequency	Fsw=10 kHz
LCL-Filter capacitance	C=2.35µF
Inverter Side Inductance	Li=3.6 mH
Grid Side Inductance	Lg=750µH

The results of the injected powers and current in both strategies are given in Fig. 5. To see the response, a voltage sag occurs with 0.65 per unit. In addition, the performance of the proposed controller in terms of overshoot and dynamic response is shown in Fig. 5. The amplitude of the voltage sag is 0.65 pu. According to the constant peak current strategy, the required average active power P^* should be 465 W and the average of reactive power Q^* should be 454 Var during the LVRT. Also according to the constant active power strategy, the required average of active power P^* should be 1000 W and the average reactive power Q^* should be 454 Var during the LVRT. After the fault is cleared, the control system quickly put the PV system into the first condition as before the fault (unity power factor) as it can be seen in Fig. 5.

VI. CONCLUSION

In this paper, a simple Model Predictive Control (MPC) was introduced. One of the most important factor for PV systems is supporting the LVRT capability. Therefore, the proposed controller was implemented for two reactive power injection strategies. The proposed controller was tested for a HERIC inverter which is one of the most popular single phase transformerless structures. The results show that the proposed controller is fast in tracking the references at fault time and is robust in the LVRT duration and also has a soft behavior with low overshoot at fault and clearance time.

REFERENCES

[1] "Global market outlook for photovoltaics 2014-2018," [Online]. Available: http://resources.solarbusinesshub.com.

[2] R. Tonkoski, D. Turcotte and T. H. M. EL-Fouly, "Impact of high PV penetration on voltage profiles in residential neighborhoods," *IEEE Trans. Sustain. Energy.,* vol. 3, no. 3, pp. 518-527, Jul. 2012.

[3] R. I. Bojoi, L. R. Limongi, D. Roiu and A. Tenconi, "Enhanced power quality control strategy for single-phase inverters in distributed generation systems," *IEEE Trans. Power Electron*., vol. 26, no. 3, pp. 798-806, Mar. 2011.

[4] X. Liang, "Emerging power quality challenges due to integration of renewable energy sources," *IEEE Trans. Ind. Appl.,* vol. 53, no. 2, pp. 855-866, Mar-Apr. 2017.

[5] N. P. Papanikolaou, "Low-voltage ride-through concept in flyback inverter-based alternating current-photovoltaic modules,"*IEEE Trans. Power Electron*., vol. 6, no. 7, pp. 1436-1448, Aug. 2013.

[6] Y. Bae, T.-K. Vu, and R.-Y. Kim, "Implemental control strategy for grid stabilization of grid-connected PV system based on German grid code in symmetrical low-to-medium voltage network," *IEEE Trans. Energy Convers.,* vol. 28, no. 3, pp. 619-631, Sept. 2013.

[7] K. J. P. Macken, M. H. J. Bollen and R. M. Belmans, "Mitigation of voltage dips through distributed generation systems." *IEEE Trans. Ind. Appl.,* Vol. 40, No. 6, Nov. 2004.

[8] Y. Q. Zhan, S. S. Choi, and D. Mahinda Vilathgamuwa "A voltage-sag compensation scheme based on the concept of power quality control center," *IEEE Trans. Power Del*., Vol. 21, No. 1, Jan. 2006.

[9] Y. Yang, H. Wang and F. Blaabjerg, "Reactive power injection strategies for single-phase photovoltaic systems considering grid requirements," *IEEE Trans. Ind. Appl*., vol. 50, no. 6, pp. 4065-4076, Nov.-Dec. 2014.

[10] A. Marinopoulos, F. Papandrea, M. Reza, S. Norrga, F. Spertino and R. Napoli, "Grid integration aspects of large solar PV installations: LVRT capability and reactive power/voltage support requirements," *Proc. of 2011 IEEE Trondheim PowerTech*, Trondheim, 2011, pp. 1-8.

[11] Y. Yang, F. Blaabjerg and Z. Zou, "Benchmarking of grid fault modes in single-phase grid-connected photovoltaic systems," *IEEE Trans. Ind. Appl.,* vol. 49, no. 5, pp. 2167-2176, Sept.-Oct. 2013.

[12] Y. Yang and F. Blaabjerg, "Synchronization in single-phase grid-connected photovoltaic systems under grid faults," *Proc. of 2012 3rd IEEE International Symposium on Power Electronics for Distributed Generation Systems (PEDG)*, Aalborg, 2012, pp. 476-482.

[13] T. Neumann and I. Erlich, "Modelling and control of photovoltaic inverter systems with respect to German grid code requirements," *Proc. of 2012 IEEE Power and Energy Society General Meeting*, San Diego, CA, 2012, pp. 1-8.

[14] Y. Yang, F. Blaabjerg and H. Wang, "Low-voltage ride-through of single-phase transformerless photovoltaic inverters," *IEEE Trans. Ind. Appl*., vol. 50, no. 3, pp. 1942-1952, May-Jun. 2014.

[15] R. Gonzalez, J. Lopez, P. Sanchis and L. Marroyo, "Transformerless inverter for single-phase photovoltaic systems," *IEEE Trans. Power Electron*., vol. 22, no. 2, pp. 693-697, Mar. 2007.

[16] B. Ji, J. Wang and J. Zhao, "High-efficiency single-phase transformerless PV h6 inverter with hybrid modulation method," *IEEE Trans. Ind. Electron.,* vol. 60, no. 5, pp. 2104-2115, May. 2013.

[17] M. Liserre, F. Blaabjerg, and S. Hansen, "Design and control of an LCL filter-based three-phase active rectifier," *IEEE Trans. Ind. Appl*., vol. 41, no. 5, pp. 1281–1291, Sep./Oct. 2005.

[18] E. Ebrahimzadeh, F. Blaabjerg, X. Wang, and C. Leth Bak, "Harmonic stability and resonance analysis in large PMSG-based wind power plants," early access in IEEE Trans. Sustain. Energy, 2017, doi: 10.1109/TSTE.2017.2712098

[19] E. Ebrahimzadeh, S. Farhangi, H. Iman-Eini, and F. Blaabjerg, "Modulation technique for four-leg voltage source Inverter without a look-up table,"IET Power Electron., vol. 9, no. 4, pp. 648-656, Mar. 2016.

[20] E. Zangeneh, S. M. Sadeghzadeh, E. Ebrahimzadeh, and F. Blaabjerg "A novel model predictive control for single-phase grid-connected photovoltaic inverters" IEEE ECCE Conference, 2017, pp. 1-7.

[21] Grid Code—High and Extra High Voltage. Bayreuth, Germany: E. ON GmbH, 2006.

[22] J. Espi, J. Castello, R. Garcia-Gil, G. Garcera, and E. Figueres, "An adaptive robust predictive current control for three-phase grid-connected inverters," *IEEE Trans. Ind. Electron.,* vol. 58, no. 8, pp. 3537–35

[23] J. W. Choi, Y. K. Kim and H. G. Kim, "Digital PLL control for single-phase photovoltaic system," *IEE Proceedings - Electric Power Applications*, vol. 153, no. 1, pp. 40-46, 1 Jan. 2006.

46, Aug. 2011.